Mathematical Biosciences and Engineering

http://www.aimspress.com/journal/mbe

MBE, 19(3): 2913–2934.
DOI: 10.3934/mbe.2022134
Received: 29 October 2021
Revised: 15 December 2021
Accepted: 21 December 2021
Published: 17 January 2022

Research article

Coverage control of mobile sensor networks with directional sensing

Zhiyang Ju[1], Hui Zhang[1,2,*], Ying Tan[3] and Xiang Chen[4]

[1] School of Transportation Science and Technology, Beihang University, Beijing 100191, China
[2] Ningbo Institute of Technology (NIT), Beihang University, Ningbo 315323, China
[3] Department of Mechanical Engineering, University of Melbourne, Melbourne, VIC 3010, Australia
[4] Department of Electrical and Computer Engineering, University of Windsor, Windsor, ON N9B 3P4, Canada

* **Correspondence:** Email: huizhang285@gmail.com.

Abstract: Control design of mobile sensors for coverage problem is addressed in this paper. The mobile sensors have non-linear dynamics and directional sensing properties which mean the sensing performance is also affected by the pointing directions of the sensors. Different from the standard optimal coverage problem where sensors are assumed to be omni-directional ones, orientation angles of the directional sensors should also be controlled, other than the position control, to achieve the coverage purpose. Considering also the non-linear dynamics of the mobile sensors, new control methodology is necessarily developed for the coverage problem with directional sensors. In the approach proposed, an innovative gradient based non-smooth motion controller is designed for the mobile sensors with unicycle dynamics. With the proposed controllers, the states of sensors will always stay in an positive invariant set where the gradient of the performance valuation function is well-defined if they are initialized within this set. Moreover, the sensors' states are proved to converge to some critical point where the gradient is zero. Simulation results are provided to illustrate the performance of the proposed coverage control strategy.

Keywords: coverage control; sensor networks; directional sensors; gradient-based control; distributed control

1. Introduction

Coverage control is one of the commonly encountered problems in mobile sensor networks [1, 2], where the mobile sensors are deployed to cover a given area to provide services such as monitoring and wireless communication [3–5]. In the literature, there are two types of coverage control problems, namely, dynamic and static coverage control. In dynamic coverage control, the purpose is to sweep

an area such that each point concerned is explored by the sensors during the movement [6, 7]. In this paper, however, the static coverage control problem [8–12] is addressed, where the control laws are designed to drive the mobile sensors from initial configuration to another configuration to cover a given area meanwhile optimizing coverage performance. In coverage control problem, the sensor types and dynamics are critical for developing control strategies. Considering sensor types, commonly addressed sensors are omni-directional sensors the coverage performance of which is not affected by the pointing directions. Plentiful coverage control work focuses on such sensors. In [10, 11, 13–15], homogeneous omni-directional sensing ranges are assumed for sensors, which means the sensors have the same sensing capability. To relax the homogeneity assumption, heterogeneous sensing ranges are also addressed in coverage control, see, for example [16–18]. Other than the continuous coverage control in the above mentioned results, discretized implementations of coverage control algorithms are also proposed in [19, 20]. In coverage control with omni-directional sensors, the sensing ranges are typically modelled as disks such that the sensing performance regarding a point is only influenced by the distance to the sensors. However, in many application scenarios, omni-directional sensing model cannot well describe the sensing performance of sensors such as cameras, infrared sensors, ultrasound sensors, and radars [21]. These sensor are termed as directional sensors in this paper, which indicates the sensing performance of a sensor is also affected by its orientation angle.

There are limited research on coverage control of mobile directional sensors [22, 23]. In this type of the problem, the sensing ranges are modelled as circular sectors [22] or ellipses [23]. With these sensing models, the simple form of typical coverage problem will be destructed, which results in difficulties in computation of gradients and designing coverage controllers. For example, the sensing models such as the circular sector result in non-smooth sensing boundaries [22]. In the following, the typical gradient-based coverage control design is described and the problem encountered with directional sensors will then be presented.

The widely used coverage control algorithm is designed based on gradients of some sensing performance valuation functions. In the scenarios with omni-directional sensors, the value function is only determined by the positions of sensors. It is shown that the gradient of the value function always exists as long as there does not exist two sensor initially at the same position. In another word, the non-differentiable configurations of the sensors' states can be naturally avoided [10, 11, 16]. However, the non-smooth sensing range such as the circular sector makes the non-differentiable scenarios more complex, which needs careful design to avoid these configurations. In our previous work [24], this issue is dealt with by approximating the non-smooth sensing range boundaries. Through this approach, the configurations of sensors where the gradient of the performance valuation function is difficult to be defined are avoided under the designed motion control. Due to the complicated computation of gradients and the approximation nature in the above approach, we use another approach in this paper to deal with the issue just mentioned. In such an approach, the configurations of sensors where the gradients are not well defined will be avoided by incorporating an artificial potential function in the coverage valuation function. Moreover, rigorous analysis of gradient computation and convergence property of the coverage control will be included.

As the coverage performance with directional sensors is determined by both the positions and pointing directions of the sensors, a ubiquitous model to describe such dynamics is unicycle model [25]. Compared to the typically used single-integral model as in [11, 15, 16], an appropriate gradient-based coverage control design is much harder as such a model is nonholonomic. Considering the difficulties

caused by directional sensing ranges and the dynamics of the mobile sensors, this paper aims to design a coverage control law for mobile sensors with directional sensing characteristics.

The sensing range of the directional sensors is modelled as circular sector which is as also pointed out in [22,24,26]. To solve the coverage problem, an artificial potential function component is added to the coverage performance valuation function in order to avoid non-differentiable configurations. Based on the gradient of the value function, an innovative non-smooth controller is developed to steer the positions and orientations of the mobile sensors to improve the corresponding coverage performance. Moreover, in order to solve the coverage problem distributedly [9–12], an improved area partition is also defined.

Considering the points mentioned above, the novelty and contributions of this paper are summarized as follows:
1) An optimization problem is constructed to model a novel coverage problem of mobile sensors subject to directional sensing ranges and unicycle dynamics.
2) An innovative distributed gradient-based coverage control algorithm is proposed for the sensors, and its convergence property is rigorously analysed. Moreover, the corresponding gradients are rigorously defined and analysed.
3) By including an artificial potential function component in the coverage performance function, an innovative strategy is developed to avoid the configurations where gradients of the performance function are not properly defined.

The remaining of the paper is organised as follows. Coverage control problem formulation with directional sensors is presented in Section 2. A partition with considering directional sensing characteristics is defined in Section 3. In Section 4, a potential function is adopted to avoid the non-differentiable cases of the performance value function. Computation of gradients is presented in Section 5. Based on the gradients, controller design for the mobile sensors and the corresponding convergence analysis is shown in Section 6. Simulation results are provided in Section 7 to illustrate the coverage performance of the proposed control algorithm. Section 8 concludes the paper and provides some possible future research directions.

2. Problem formulation

In this paper, a group of mobile sensors are responsible for covering a given compact area $V \in \mathbb{R}^2$. The set of the sensors' indices is denoted as $\mathcal{N} = \{1, \ldots, n\}$ with n being the total number of sensors. As illustrated in Figure 1, the position of sensor i is denoted by $p_i = \begin{bmatrix} x_i & y_i \end{bmatrix}^\mathsf{T}$ with x_i, y_i being the coordinates in a given coordinate system XOY. The orientation angle of sensor i is represented by θ_i with positive values indicating counter-clockwise directions. In this paper, unicycle dynamics is assumed for the sensors, which is expressed as

$$\begin{aligned} \dot{x}_i &= v_i \cos\theta_i, \\ \dot{y}_i &= v_i \sin\theta_i, \\ \dot{\theta}_i &= \omega_i, \end{aligned} \tag{2.1}$$

where v_i is the longitudinal speed of sensor i, and ω_i denotes its angular velocity. Here, v_i and ω_i are the inputs for sensor i. In the rest of the paper, states of sensor i are denoted as $z_i = \begin{bmatrix} x_i & y_i & \theta_i \end{bmatrix}^\mathsf{T}$. The

sensing range of each sensor is a circular sector denoted as S_i with a centrally spanned angle α and a radius R as in Figure 1.

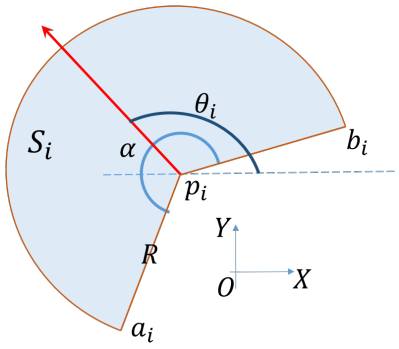

Figure 1. Sensing range of the i^{th} agent.

In this figure, XOY frame denotes the global coordinate system where the positions and the heading angles of sensors are defined. In the considered coverage control problem, the mobile sensors are assumed to have identical sensing ranges. The sensing range is bounded by two line segments p_ia_i and p_ib_i and an arc $\overset{\frown}{a_ib_i}$. Note that when $R = \infty$, the boundaries are only two lines p_ia_i and p_ib_i. The area outside the sensing range (or boundaries) is the dead sensing zone where targets in this area cannot be sensed. For instance, the sensing range of a camera with fish-eye lens can be modelled as such a directional range [22].

2.1. Sensing performance of mobile sensors

The control objective of the coverage problem is to steer a group of mobile sensors to optimize the sensing performance regarding a given region. A value function $f(z_i, q)$ is used to evaluate the coverage performance of sensor i regarding a target point $q = \begin{bmatrix} q_x & q_y \end{bmatrix}^\mathsf{T}$ in the given area $V \in \mathbb{R}^2$. This function not only is related to sensor i's position but also its orientation angle as the directional sensing characteristics.

Inspired by the work in [22, 26] and coverage problem with omni-directional sensors [9–11], two principles are generally taken into consideration to select an appropriate $f(z_i, q)$. One is that the function $f(z_i, q)$ is non-negative and its value is 0 if and only if q is in the dead sensing zone of sensor i. The other one is that the sensing performance degrades as the distance between q and p_i increases. Considering these two principles, the following performance value function is adopted:

$$f(z_i, q) = e^{-\frac{\sqrt{(q_x - x_i)^2 + (q_y - y_i)^2}}{D}} \mathbf{1}_{S_i}(q), \tag{2.2}$$

where $\mathbf{1}_{S_i}(q)$ is the indicator function with its value being 1 if $q \in S_i$ and 0, otherwise, and D is a positive design parameter with $\frac{1}{D}$ denoting the decaying rate of sensing performance regarding the distance to the sensors. For convenience of presentation, we also denote $e^{-\frac{\sqrt{(q_x - x_i)^2 + (q_y - y_i)^2}}{D}}$ as $g(p_i, q)$.

Remark 1. In the coverage control problem with omni-directional sensors, the value of the sensing performance function is only determined by the distances between a point and the sensors [11, 16]. When the sensors are with directional sensing ranges as in this paper, the sensing performance is also

affected by the orientation angles of sensors. Other than the sensing performance model in this paper, other models to describe the directional sensing characteristics can also be found in [22, 23] ∘

As the derivatives corresponding to S_i's boundaries will be used later for gradient computation. We now provide the mathematical expressions of them. The boundaries p_ia_i and p_ib_i (see Figure 1 for more details) are specifically expressed as

$$\begin{aligned} p_ia_i : \begin{bmatrix} x & y \end{bmatrix}^\mathsf{T} &= \Re(\theta_i + \frac{\alpha}{2}) \begin{bmatrix} \tau & 0 \end{bmatrix}^\mathsf{T} + p_i, \tau \in [0, R], \\ p_ib_i : \begin{bmatrix} x & y \end{bmatrix}^\mathsf{T} &= \Re(\theta_i - \frac{\alpha}{2}) \begin{bmatrix} \tau & 0 \end{bmatrix}^\mathsf{T} + p_i, \tau \in [0, R], \end{aligned} \tag{2.3}$$

where x, y denote the coordinates of points on the corresponding boundaries and $\Re(\theta)$ is defined as $\Re(\theta) := \begin{bmatrix} \cos\theta & -\sin\theta \\ \sin\theta & \cos\theta \end{bmatrix}$. Moreover, the points on boundary $\widehat{a_ib_i}$ are defined as

$$\begin{bmatrix} x & y \end{bmatrix}^\mathsf{T} = \begin{bmatrix} R\cos(\theta_i + \sigma) & R\sin(\theta_i + \sigma) \end{bmatrix}^\mathsf{T} + p_i, \sigma \in [-\frac{1}{2}\alpha, \frac{1}{2}\alpha]. \tag{2.4}$$

With the sensing performance value for each individual sensor defined, the coverage value function considering all sensors regarding the given area V is constructed as

$$H_1(Z) = \int_V \max_{i \in \mathcal{N}} f(z_i, q) dq, \tag{2.5}$$

where Z denotes the stack of states of all sensors, which is $Z = \begin{bmatrix} z_1^\mathsf{T} & \dots & z_n^\mathsf{T} \end{bmatrix}^\mathsf{T}$. As the states of sensors vary with time, to specifically indicate the value function at time t, it is written as $H_1(t) = H_1(Z(t)) = \int_V \max_{i \in \mathcal{N}} f(z_i, q) dq$.

The objective of the coverage control problem is to design control strategies to maximize the coverage performance value function of the sensors for a give area V. More precisely, the following static optimization of the value function is used to describe the objective:

$$\max_Z H_1(Z). \tag{2.6}$$

According to typical approaches in [10, 11], in order to design an appropriate control law that can drive the system to one of the optimal solutions or local optimal solutions of the value function $H_1(Z)$, the gradient of the value function is required to be computed. Moreover, in order to design distributed control laws, computation of gradients is also preferred to be local.

3. Partition of area V

In order to design a distributed gradient based controller, a Voronoi partition of the area V is typically employed in the literature [11, 27]. In the following, we present the partition which will be used for gradient computation in this paper and rewrite the performance value function according to the partition cells.

To address the sensing performance regarding the points in V, naturally a partition regarding $f(z_i, q), \forall i \in \mathcal{N}$ is defined as

$$V_i(Z) := \{q \in V \cap S(z_i) | f(z_i, q) \geq f(z_j, q), \forall j \in \mathcal{N}\}, Z \in \mathbb{R}^{3n} \setminus \mathcal{S}_C, \tag{3.1}$$

where S_C denotes the set of points where the partition is not properly defined, which will be analysed next, and $S(z_i)$ denotes the sensing range S_i, as in Figure 1, regarding the sensor i's state z_i. When the spanned angle α of each sensing range is 2π, S_C is the set when there exist two sensors at the same position as pointed in [13]. For a general value of α, a modified definition should be proposed with considering the directional sensing ranges of sensors.

We define a set

$$\mathcal{A}(Z) := \left\{ q \in \mathcal{V} | \exists i, j \in \mathcal{N} \text{ s.t.} q \in S(z_i) \cap S(z_j), f(z_i, q) = f(z_j, q) \geq f(z_k, q), \forall k \in \mathcal{N} \right\}, \tag{3.2}$$

which represents the set of points regarding which there are two sensors have the same sensing performance. As the partition cells $V_i, \forall i \in \mathcal{N}$ should satisfy the condition that they have disjoint interiors, the measure of set $\mathcal{A}(Z)$ shall be zero for all $Z \in \mathbb{R}^{3n} \setminus \mathcal{S}_C$. Otherwise, the partition according to the partition rule in Eq (3.1) fails, which renders the distributed calculation of gradients difficult. A case when the partition rule fails is illustrated as in Figure 2.

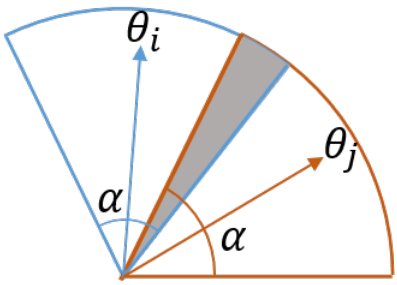

Figure 2. An example where partition $V_i, i \in \mathcal{N}$ fails.

It shows that when $\alpha < \pi$ and the angle between θ_i and θ_j is less than α, the sensing performances regarding i and j within the grey area are the same. This renders a non-zero measure of $\mathcal{A}_Z$ and thus fails the partition in Eq (3.1). When $\alpha > \pi$, it is easily to show that the partition fails when $p_i = p_j$ for some $i \neq j$. Thus, we have the following formal definition of $\mathcal{S}_C$:

$$\mathcal{S}_C := \{Z \in R^{3n} | \exists i, j \in \mathcal{N}, i \neq j \text{ s.t. } p_i = p_j, |\theta_i - \theta_j| \leq \alpha \text{ or } |\theta_i - \theta_j \pm \pi| \leq \alpha\}. \tag{3.3}$$

Note that when $\alpha > \pi$, S_C can also be written as $\mathcal{S}_C = \{Z \in \mathbb{R}^{3n} | \exists i, j \in \mathcal{N}, i \neq j \text{ s.t. } p_i =_j\}$.

Define S_I as

$$S_I := \mathbb{R}^{3n} \setminus S_C. \tag{3.4}$$

Then the partition in Eq (3.1) is properly defined on S_I and the value function $H_1(Z)$ in Eq (2.5) can be rewritten as

$$H_1(Z) = \sum_{i=1}^{n} \int_{V_i(Z)} f(z_i, q) dq, Z \in S_I. \tag{3.5}$$

It is noted that a partition cell V_i may consist of several separate planar pieces, which is caused by the directional sensing ranges, and the union of all the partition cells might not cover the whole V due to the limited sensing radius R. Thus it is slightly abuse of the term partition.

Remark 2. The idea of the partition is inspired by the Voronoi partition. However, the partition defined in this paper might not cover a given set in some cases, which is partially caused by the directional sensing ranges and slightly different from the definition of commonly used Voronoi partition in coverage problems. Readers may refer to abstract Voronoi partition as in [28] for more information.

Here we provide a definition of neighbours for further expression. The neighbourhood of sensor i regarding the proposed partition is defined as $\mathcal{N}_i =: \{j|V_i \cap V_j \neq \emptyset\}$. Moreover, we assume each sensor i can communicate with its neighbours. Based on the form of the value function as in Eq (3.5), the gradient regarding each sensor state z_i can now be computed distributedly on S_I by only using information from neighbours. However, the gradient on S_C is still difficult to define, let alone distributed computation of it. In this paper, we design artificial potential functions to generate potential field to prevent the sensors' states from entering S_C.

4. Performance value function improvement with potential function design

Due to the directional sensing ranges of sensors, the set S_C in which the gradients of the value function are not properly defined cannot be naturally avoided as in the omni-directional sensor coverage problem [15]. Thus artificial potential functions are designed to prevent sensors' states from entering S_C. Another benefit brought by such an approach is collision avoidance of sensors as in real applications the sensors possibly collide with each other though their sizes are small compared to the size of the area to be covered. In the following, first the potential functions is presented. Then the performance value function is modified by incorporating the potential functions.

Remark 3. Another strategy to avoid the configurations where the gradient of the value function is not properly defined is proposed in our previous work in [24]. In this strategy, the straight line boundaries of the sensing ranges S_i are approximated by some properly designed curves and sensing performance function is also slightly modified, which leads to positive invariant property of the set S_I when a gradient based coverage controller is applied on sensors.

To avoid set S_C, an artificial potential function is adopted for each pair of sensors to repel them away from each other, which is

$$h_{ij}(Z(t)) := \begin{cases} \frac{1}{2}\eta(\frac{1}{\|p_i - p_j\|} - \frac{1}{\rho_0})^2 & \text{if } \|p_i - p_j\| \leq \rho_0, \\ 0 & \text{if } \|p_i - p_j\| > \rho_0, \end{cases} \tag{4.1}$$

where η and ρ_0 are positive constants to be selected. In implementation, ρ is usually selected to be slightly larger than the size of the sensors in order to avoid collision and reduce the influence of the potential functions on coverage performance at the same time. For instance, if the sensors are in a disc shape, ρ can be a value which is slightly larger than the disc's radius. For the same purpose, μ is usually selected to be small and can be selected from the interval $[0.1, 1]$. Based on the definition of the potential functions, a graph $G^p(Z) = (\mathcal{N}, \mathcal{E}^p(Z))$ is induced with $\mathcal{E}^p(Z) := \{\{i, j\}|\|p_i - p_j\| \leq \rho_0\}$ and the neighbourhood of sensor i regarding G^p is defined as $\mathcal{N}_i^p = \{j|\{i, j\} \in \mathcal{E}^p\}$. By incorporating the artificial potential functions into the performance function, a new performance function is constructed as

$$H(Z) = H_1(Z) + H_2(Z), \tag{4.2}$$

where

$$H_2(Z) := -\sum_{\{i,j\}\in\mathcal{E}^p(Z)} h_{i,j}(Z). \tag{4.3}$$

As the control objective is to maximize the value function, the negative sign in Eq (4.3) implies the gradient direction of H_2 is along the direction of increasing the distances between sensors. In Section 6, it will be shown that the designed gradient based controller based on the performance valuation function $H(Z)$ keep the sensors' states from entering S_C.

5. Computation of gradients

Distributed computation of gradients of $H(Z)$ in S_I with respect to sensors' states are presented in the following based on the partition in Eq (3.1).

To help present computation of the gradients of $H(Z)$, several sets are first defined. We use ∂V_i and ∂S_i to denote the boundaries of the areas V_i and S_i, respectively, ∂S_i^B is defined as $\partial S_i^B := p_i a_i \cup p_i b_i$ and ∂S_i^C represents the set of points on the arc part of S_i's boundary, which is $\partial S_i^C = \partial S_i \setminus \partial S_i^B$. The partial derivatives of $H(Z)$ with respect to sensors' states can be locally computed as

$$\begin{aligned}\frac{\partial H}{\partial x_i} =& \frac{\partial \int_{V_i} g(p_i,q)dq}{\partial x_i} + \sum_{j\in\mathcal{N}_i}\frac{\partial \int_{V_j} g(p_j,q)dq}{\partial x_i} + \sum_{j\in\mathcal{N}_i^p}\frac{\partial h_{ij}(Z)}{\partial x_i}\\ =& \int_{V_i}\frac{\partial g(p_i,q)}{\partial x_i}dq + \int_{\partial V_i\cap\partial S_i^C} g(p_i,q)\frac{\partial s}{\partial x_i}^{\mathsf{T}}\mathbf{n}ds + \int_{\partial V_i\cap\partial S_i^B} g(p_i,q)\frac{\partial s}{\partial x_i}^{\mathsf{T}}\mathbf{n}ds\\ &+ \sum_{j\in\mathcal{N}_i}\int_{\partial V_j\cap\partial S_i^B} g(p_j,q)\frac{\partial s}{\partial x_i}^{\mathsf{T}}\mathbf{n}ds + \sum_{j\in\mathcal{N}_i^p}\eta\left(\frac{1}{\|p_i-p_j\|}-\frac{1}{\rho_0}\right)\frac{x_i-x_j}{\|p_i-p_j\|^3},\end{aligned} \tag{5.1}$$

$$\begin{aligned}\frac{\partial H}{\partial y_i} =& \frac{\partial \int_{V_i} g(p_i,q)dq}{\partial y_i} + \sum_{j\in\mathcal{N}_i}\frac{\partial \int_{V_j} g(p_j,q)dq}{\partial y_i} + \sum_{j\in\mathcal{N}_i^p}\frac{\partial h_{ij}(Z)}{\partial x_j}\\ =& \int_{V_i}\frac{\partial g(p_i,q)}{\partial y_i}dq + \int_{\partial V_i\cap\partial S_i^C} g(p_i,q)\frac{\partial s}{\partial y_i}^{\mathsf{T}}\mathbf{n}ds + \int_{\partial V_i\cap\partial S_i^B} g(p_i,q)\frac{\partial s}{\partial y_i}^{\mathsf{T}}\mathbf{n}ds\\ &+ \sum_{j\in\mathcal{N}_i}\int_{\partial V_j\cap\partial S_i^B} g(p_j,q)\frac{\partial S}{\partial y_i}^{\mathsf{T}}\mathbf{n}ds + \sum_{j\in\mathcal{N}_i^p}\eta\left(\frac{1}{\|p_i-p_j\|}-\frac{1}{\rho_0}\right)\frac{y_i-y_j}{\|p_i-p_j\|^3},\end{aligned} \tag{5.2}$$

$$\begin{aligned}\frac{\partial H}{\partial \theta_i} =& \frac{\partial \int_{V_i} g(p_i,q)dq}{\partial \theta_i} + \sum_{j\in\mathcal{N}_i}\frac{\partial \int_{V_j} g(p_j,q)dq}{\partial \theta_i}\\ =& \int_{V_i}\frac{\partial g(p_i,q)}{\partial \theta_i}dq + \int_{\partial V_i\cap\partial S_i^C} g(p_i,q)\frac{\partial s}{\partial \theta_i}^{\mathsf{T}}\mathbf{n}ds + \int_{\partial V_i\cap\partial S_i^B} g(p_i,q)\frac{\partial s}{\partial \theta_i}^{\mathsf{T}}\mathbf{n}ds\\ &+ \sum_{j\in\mathcal{N}_i}\int_{\partial V_j\cap\partial V_i^B} g(p_j,q)\frac{\partial s}{\partial \theta_i}^{\mathsf{T}}\mathbf{n}ds,\end{aligned} \tag{5.3}$$

where s parameterizes the corresponding boundary and $\mathbf{n}$ denotes the outward unit normal of the corresponding boundary. Note that s and n have different expressions for different boundaries. We show the derivation of these partial derivatives in the proof of Proposition 1.

Proposition 1. *Assume the boundary of V is a simple closed curve. Given the performance function f, the function g and potential functions $h_{i,j}(Z), \forall\{i,j\} \in \mathcal{E}^p(Z)$, the value function $H(Z)$ is continuous differentiable on S_I, where for each $i \in \mathcal{N}$ the partial derivatives are computed as in Eqs (5.1)–(5.3).*

Proof. According to the definition, $g(p_i, q)$ is continuously differentiable with respect to (p_i, q) for $p_i \in \mathbb{R}^3$ and $q \in V_i(P)$, $\forall i \in \mathcal{N}$. Thus, both $f(z_i, q)$ and $\frac{\partial g(p_i,q)}{\partial Z}$ are integrable on $V_i(Z)$ for each $i \in \mathcal{N}$ and $Z \in S_I$.

If $Z \notin S_C$, the set $\mathcal{A}(Z)$ has measure zero. As the boundaries of $S_i, \forall i \in \mathcal{N}$ are finite number of straight lines and arcs and the common boundaries between any two sensors' ranges are finite number of straight lines, it can be concluded that $V_i(Z)$ has finite number of separate subsets $\forall Z \in S_I, \forall i \in \mathcal{N}$. Based on the above two facts, $\{V_i(Z)|Z \in S_I\}$ is a piecewise smooth family for each $i \in \mathcal{N}$. Now, we can apply the differentiation process as in [29].

First the partial derivatives of $H_1(Z)$ are considered. For each $i \in \mathcal{N}$, we have

$$\frac{\partial H_1(Z)}{\partial x_i} = \frac{\partial \int_{V_i} g(p_i, q)dq}{\partial x_i} + \sum_{j\in\mathcal{N}_i} \frac{\partial \int_{V_j} g(p_j, q)dq}{\partial x_i}. \tag{5.4}$$

Now, we consider the partial derivative at a point Z_0. The corresponding entries of Z_0 are similarly denoted as $x_{i,0}$, $y_{i,0}$, $\theta_{i,0}$ and $p_{i,0} = \begin{bmatrix} x_{i,0} & y_{i,0} \end{bmatrix}^\mathsf{T}$. By chain rule, the first term on the right hand side in Eq (5.4) is expressed as

$$\frac{\partial \int_{V_i} g(p_i, q)dq}{\partial x_i}\Big|_{Z=Z_0} = \int_{V_i(Z_0)} \frac{\partial g(x_i, y_{i,0}, q)}{\partial x_i}\Big|_{x_i=x_{i,0}} dq + \frac{d}{dx_i} \int_{V_i(Z_{0,x_i})} g(p_{i,0}, q)dq\Big|_{x_i=x_{i,0}}, \tag{5.5}$$

where $g(x_i, y_{i,0}, q) = g(\hat{p}_{i,0}, q)$ with $\hat{p}_{i,0} := \begin{bmatrix} x_i & y_{i,0} \end{bmatrix}^\mathsf{T}$ and Z_{0,x_i} denotes the vector whose entries are the same as Z_0 expect for the entry $x_{i,0}$ which replaces x_i. Inspired by the derivation in [29], the second term on the right hand side of Eq (5.5) is computed as

$$\begin{aligned}
&\frac{d}{dx_i} \int_{V_i} g(p_{i,0}, q)dq\Big|_{x_i=x_{i,0}} = \int_{\partial V_i} g(p_{i,0}, q) \frac{\partial s^\mathsf{T}}{\partial x_i}\Big|_{x_i=x_{i,0}} \mathbf{n}ds \\
&= \int_{\partial V_i \cap \partial V} g(p_{i,0}, q) \frac{\partial s^\mathsf{T}}{\partial x_i}\Big|_{x_i=x_{i,0}} \mathbf{n}ds + \sum_{j\in\mathcal{N}_i(Z_0)} \int_{\partial V_i \cap \partial V_j} g(p_{i,0}, q) \frac{\partial s^\mathsf{T}}{\partial x_i}\Big|_{x_i=x_{i,0}} \mathbf{n}ds \\
&\quad + \int_{(\partial V_i \setminus \partial V) \setminus (\bigcup_{j\in\mathcal{N}_i(Z_0)} \partial V_j)} g(p_{i,0}, q) \frac{\partial s^\mathsf{T}}{\partial x_i}\Big|_{x_i=x_{i,0}} \mathbf{n}ds \\
&= \sum_{j\in\mathcal{N}_i(Z_0)} \int_{\partial V_i \cap \partial V_j} g(p_{i,0}, q) \frac{\partial s^\mathsf{T}}{\partial x_i}\Big|_{x_i=x_{i,0}} \mathbf{n}ds + \int_{(\partial V_i \setminus \partial V) \setminus (\bigcup_{j\in\mathcal{N}_i(Z_0)} \partial V_j)} g(p_{i,0}, q) \frac{\partial s^\mathsf{T}}{\partial x_i}\Big|_{x_i=x_{i,0}} \mathbf{n}ds,
\end{aligned} \tag{5.6}$$

where the last equality is established with the fact that ∂V does not vary with Z and $V_i(Z_{0,x_i})$ is simplified as V_i for expression convenience.

With similar derivation, as $\frac{\partial g(p_{j,0},q)}{\partial x_i} = 0$, each summand in the second term on the right hand side of Eq (5.4) can be written as

$$\frac{\partial \int_{V_j} g(p_j,q)dq}{\partial x_i}\Big|_{Z=Z_0} = \frac{d}{dx_i}\int_{V_j(Z_{0,x_i})} g(p_{j,0},q)dq = \int_{\partial V_j\cap\partial V_i} g(p_{j,0},q)\frac{\partial s^{\mathsf{T}}}{\partial x_i}\Big|_{x_i=x_{i,0}}\mathbf{n}ds. \tag{5.7}$$

On the boundary segments $(\partial V_i \cap \partial V_j) \cap \partial S_i^B$, for each $j \in \mathcal{N}_i$, it is easily to check that $g(p_{i,0},q) = g(p_{j,0},q)$ for all q on such segments based on the definition of the partition Eq (3.1), and the two corresponding outward unit normal point opposite directions. Thus the integral terms regarding these segments in Eqs (5.6) and (5.7) will cancel each other when they are substituted into Eq (5.4). Substitute Eq (5.6) into (5.5) and substitute Eqs (5.5) and (5.7) into (5.4), and apply the above deduction processes to every $Z \in S_I$, the partial derivative of $H_1(Z)$ with respect to x_i is computed as

$$\begin{aligned}\frac{\partial H_1(Z)}{\partial x_i} = &\int_{V_i}\frac{\partial g(p_i,q)}{\partial x_i}dq + \int_{\partial V_i\cap\partial S_i^C} g(p_i,q)\frac{\partial s}{\partial x_i}^{\mathsf{T}}\mathbf{n}ds + \int_{\partial V_i\cap\partial S_i^B} g(p_i,q)\frac{\partial s}{\partial x_i}^{\mathsf{T}}\mathbf{n}ds\\ &+\sum_{j\in\mathcal{N}_i}\int_{\partial V_j\cap\partial S_i^B} g(p_j,q)\frac{\partial s}{\partial x_i}^{\mathsf{T}}\mathbf{n}ds.\end{aligned} \tag{5.8}$$

Similar results can be achieved for the partial derivatives with respect to y_i and θ_i for all $i \in \mathcal{N}$.

With the definition of H_2 and h_{ij}, it is easy to conclude that $H_2(Z)$ is continuously differentiable on S_I. The partial derivative of $H_2(Z)$ with respect to x_i is expressed as

$$\frac{\partial H_2(Z)}{\partial x_i} = \sum_{j\in\mathcal{N}_i^p}\eta\left(\frac{1}{\|p_i-p_j\|}-\frac{1}{\rho_0}\right)\frac{x_i-x_j}{\|p_i-p_j\|^3}. \tag{5.9}$$

Combining Eqs (5.8) and (5.9), the partial derivative in Eq (5.1) is established. Similarly, the partial derivatives in Eqs (5.2) and (5.3) can also be achieved with just noting that $\frac{\partial H_2(Z)}{\partial \theta_i} = 0$. □

Note that in the case when the sensing radius R is infinity, the integral terms regarding $\partial V_i \cap \partial S_i^C$ shall be zero in the partial derivatives. Each point on the boundary ∂S_i^B, which is defined in Eq (2.3), can further be expressed as:

$$s = p_i + \rho(s)\begin{bmatrix}\cos(\theta_i+\epsilon(s))\\ \sin(\theta_i+\epsilon(s))\end{bmatrix},$$

where $\rho(s) \in [0,R]$ and $\epsilon(s) \in \{-\frac{1}{2}\alpha, \frac{1}{2}\alpha\}$ are neither depend on states of sensors. Thus, the partial derivatives of s with respect to z_i are expressed as

$$\frac{\partial s}{\partial x_i} = \begin{bmatrix}1\\0\end{bmatrix},\ \frac{\partial s}{\partial y_i} = \begin{bmatrix}0\\1\end{bmatrix},\ \frac{\partial s}{\partial \theta_i} = \rho(s)\begin{bmatrix}-\sin(\theta_i+\epsilon(s))\\ \cos(\theta_i+\epsilon(s))\end{bmatrix} = \begin{bmatrix}0 & -1\\ 1 & 0\end{bmatrix}(s-p_i). \tag{5.10}$$

The outward unit $\mathbf{n}$ on the boundary p_ia_i as expressed in Eq (2.3) is calculated as

$$\mathbf{n} = \Re(\theta_i+\frac{1}{2}\alpha)\begin{bmatrix}1 & 0\end{bmatrix}^{\mathsf{T}}, \tau \in (0,R), \tag{5.11}$$

where $\Re(\theta)$ is defined in Eq (2.3). Similarly, the outward unit on the boundary p_ib_i is calculated as

$$\mathbf{n} = \Re(\theta_i-\frac{1}{2}\alpha)\begin{bmatrix}1 & 0\end{bmatrix}^{\mathsf{T}}, \tau \in (0,R). \tag{5.12}$$

According to the expression in Eq (2.4), the partial derivatives of any s on S_i^C are the same as in Eq (5.10), and the outward unit at a point s on the boundary S_i^C is determined as

$$\mathbf{n} = \frac{s - p_i}{\|s - p_i\|}. \tag{5.13}$$

By substituting Eqs (5.10)–(5.13) into (5.1)–(5.3), the partial derivatives of $H(Z)$ with respect to each z_i can be calculated and directly implemented.

6. Gradient-based coverage controllers

Based on the gradients calculated in Eq (5.1)–(5.3), an innovative controller is designed for each mobile sensor to optimize the coverage performance of the given area V. This section presents the controller design and the convergence analysis.

6.1. Controller design of mobile sensors

In most of the coverage control literature such as [15, 22, 23], the control of positions and orientation angles of sensors are decoupled due to simple dynamics. However, in the dynamics of sensors in Eq (2.1), position and orientation angle control are coupled. Thus new controllers are needed to be designed using the gradient information of $H(Z)$ to maximize the performance function. It is noted that the dynamics of sensors presented is nonholonomic. Such systems do not satisfy Brocketts necessary smooth feedback stabilization condition [30]. In order to achieve the optimal performance with respect to the value function $H(Z)$, the following non-smooth distributed gradient-based control law is proposed for the i^{th} sensor:

$$\begin{aligned} v_i =& k\frac{\partial H(Z)}{\partial x_i}\cos(\theta_i) + k\frac{\partial H(Z)}{\partial y_i}\sin(\theta_i), \\ \omega_i =& 2k_1 g_i(Z) sign\left(\frac{\partial H(Z)}{\partial \theta_i}\right) + k_2\frac{\partial H(Z)}{\partial \theta_i}, \end{aligned} \tag{6.1}$$

where $sign(x) = -1$ if $x < 0$ and $sign(x) = 1$ if $x \geq 0$, $k > 0$, $k_1 > 0$ and $k_2 > 0$ are tuning parameters and $g_i(Z)$ is defined as

$$g_i(Z) := \left| \arctan\left(\frac{\begin{bmatrix} -\sin\theta_i & \cos\theta_i \end{bmatrix} \begin{bmatrix} \frac{\partial H(Z)}{\partial x_i} & \frac{\partial H(Z)}{\partial y_i} \end{bmatrix}^{\mathsf{T}}}{\begin{bmatrix} \cos\theta_i & \sin\theta_i \end{bmatrix} \begin{bmatrix} \frac{\partial H(Z)}{\partial x_i} & \frac{\partial H(Z)}{\partial y_i} \end{bmatrix}^{\mathsf{T}}} \right) \right|.$$

Remark 4. Due to the non-smooth component in the control input ω_i, chattering might happen in implementation. To alleviate such a phenomenon, a low path filter can be introduced to smooth out the control input signal with with sacrificing the performance, i.e., the states of the system might converge to a neighbourhood of the theoretical convergence point. ∘

Next, it shows that if the states of the sensors initially lie in the continuous differentially set S_I, it will stay in that set forever.

6.2. Positive invariance of S_I

To stay away from the set S_C where differentiability of $H(Z)$ is hard to analyse, we show that the set S_I is positively invariant. That is, once the initial state of sensors lies within S_I, it will stay in this set at any future time under the dynamics in Eq (2.1) and control law designed in Eq (6.1). Letting S_I be defined as in Eq (3.4), the first main result is summarized in Theorem 1.

Theorem 1. *For the dynamics Eq (2.1) with the control inputs proposed in Eq (6.1), the set S_I is positively invariant.*

Proof. For each i, denote $z_i(\cdot)$ as a Filippov solution of Eq (2.1) with the controller as in Eq (6.1), which satisfies

$$\dot{z}_i \in K[g](z_i), \tag{6.2}$$

where $g(z_i) := \begin{bmatrix} v_i \cos\theta_i \\ v_i \sin\theta_i \\ \omega_i \end{bmatrix}$ and $K[g](z_i)$ denotes the Filippov of g [31, 32]. If $Z(0) \in S_N$, according to the definition of $H(Z)$ in Eq (4.2), its derivative along the trajectories of Eq (2.1) exists as

$$\frac{d}{dt}H(Z(t)) \in \dot{\tilde{H}}(Z(t)) \tag{6.3}$$

where

$$\begin{aligned}
\dot{\tilde{H}} =& \nabla H^{\mathsf{T}} K[G](Z) \\
=& \sum_{i=1}^{n} \left[\frac{\partial H}{\partial x_i} \quad \frac{\partial H}{\partial y_i} \quad \frac{\partial H}{\partial \theta_i}\right] K\left[\begin{bmatrix} v_i \cos\theta_i & v_i \sin\theta_i & \omega_i \end{bmatrix}^{\mathsf{T}}\right] \\
=& \sum_{i=1}^{n} k\Big(\frac{\partial H}{\partial x_i}\cos\theta_i + \frac{\partial H}{\partial y_i}\sin\theta_i\Big)^2 + \Big|\frac{\partial H}{\partial \theta_i}\Big|^2 + 2k_1 \frac{\partial H}{\partial \theta_i} K\Big[g_i(Z) sign\Big(\frac{\partial H}{\partial \theta_i}\Big)\Big] \\
\subset& \sum_{i=1}^{n} k\Big(\frac{\partial H}{\partial x_i}\cos\theta_i + \frac{\partial H}{\partial y_i}\sin\theta_i\Big)^2 + \Big|\frac{\partial H}{\partial \theta_i}\Big|^2 + 2k_1 \frac{\partial H}{\partial \theta_i} SGN_i(Z),
\end{aligned} \tag{6.4}$$

where

$$SGN_i(Z) = \begin{cases} [-\frac{\pi}{2}, 0] & \frac{\partial H}{\partial \theta_i} < 0, \\ [-\frac{\pi}{2}, \frac{\pi}{2}] & \frac{\partial H}{\partial \theta_i} = 0, \\ [0, -\frac{\pi}{2}] & \frac{\partial H}{\partial \theta_i} > 0. \end{cases} \tag{6.5}$$

As each element in $\dot{\tilde{H}}$ is greater than or equal to 0, the derivative of $H(t)$ is non-negative. It can be concluded that $H(t)$ is non-increasing along the trajectory. Therefore,

$$H(t) \geq H(0), \forall t \geq 0. \tag{6.6}$$

Next, we proof the conclusion by contradiction. If there exists a time instant τ such that: as t tends to τ, $\|p_i(t) - p_j(t)\|$ tends to 0. That is, $\lim_{t\to\tau} h_(ij)(Z(t)) = \infty$. This leads to $\lim_{t\to\tau} H(t) < H(0)$, which contradicts the condition in Eq (6.6). This implies that the state $Z(t)$ cannot leave the set S_I if $Z(0) \in S_I$. Thus S_I is positively invariant. □

Define the maximum of $H_1(Z)$ as H_1^*, that is, $H_1^* = \max_{Z\in\mathbb{R}^{3n}} H_1(Z)$. Then the distance between any two sensors can be bounded below as in Proposition 2.

Proposition 2. *If $Z(0) \in S_N$, then for any $t \geq 0$,* $\max_{\{i,j\}\in\{\{i,j\}|i,j\in\mathcal{N},i\neq j\}} h_{ij}(t) \leq \frac{\rho_0\sqrt{\eta}}{\sqrt{\eta}+\rho_0\sqrt{2(H(0)-H_1^*)}}$.

Proof. From the definition of $H(t)$ in Eq (4.2), we have

$$H(t) = H_1(t) + H_2(t) \leq H_1^* + H_2(t), \forall t \geq 0. \tag{6.7}$$

At the same time, $H(t) \geq H(0)$ as in Eq (6.6). Thus,

$$\max_{\{i,j\}\in\{\{i,j\}|i,j\in\mathcal{N},i\neq j\}} h_{ij}(t) \geq H_2(t) \geq H(0) - H_1^*. \tag{6.8}$$

Based on the definition of h_{ij} in Eq (4.1), the conclusion is achieved.

□

6.3. Convergence properties of coverage control

Instead of achieving the optimal value of the coverage performance value function as in omni-directional sensor cases, the coverage control with directional sensors can only achieve local optimum of the performance function $H(Z)$ due to its non-convex feature. Denote $S_{critical} = \left\{Z \in \mathbb{R}^{3n} \,\middle|\, \frac{\partial H}{\partial Z} = 0\right\}$. With the result presented in Theorem 1, Theorem 2 shows the convergence of the closed loop system which consists of the dynamics Eq (2.1) and the control inputs proposed in Eq (6.1). More precisely, the sensors' state will asymptotically converge to $S_{critical}$.

Theorem 2. *Suppose that initial states of sensors satisfy $Z(0) \in S_I$. The states of the mobile sensor system with the sensor dynamics Eq (2.1) and the control inputs Eq (6.1) will converge to $S_{critical}$.*

Proof. As H_1 is bounded above and H_2 is negative, it is obvious that $H(Z)$ is bounded above. Denote $\bar{H}$ as an upper bound of $H(Z)$ and define V_E as $V_E(t) := \bar{H} - H(Z(t))$. Thus, $V_E(t)$ is positive definite. In the following, V_E is selected as a Lyapunov candidate. According to the derivative computation in Eq (6.3), the derivatives of V_E along the trajectories of the dynamic system (2.1) satisfies

$$\frac{dV_E}{dt} = -\frac{dH}{dt} \leq 0. \tag{6.9}$$

As V_E is bounded above, the state Z converges to a point Z^* in Ω with Ω being denoted as

$$\Omega = \left\{Z|\frac{\partial H}{\partial x_i}\cos\theta_i + \frac{\partial H}{\partial y_i}\sin\theta_i = 0, \frac{\partial H}{\partial \theta_i} = 0,\ \forall i \in \mathcal{N}\right\}.$$

Note that Ω is set of all points where $0 \in \dot{\bar{H}}(Z)$. Next we show the sensors' state will finally converge to the set of $S_{critical}$. We now focus on the states in set Ω. Two subsets of Ω are defined as

$$\mathcal{M} := \{Z|Z \in \Omega,\ \frac{\partial H}{\partial x_i} = 0,\ \frac{\partial H}{\partial y_i} = 0, \forall i \in \mathcal{N}\}$$

and

$$\mathcal{E} := \{Z|Z \in \Omega,\ \exists i \in \mathcal{N}\ s.t.\ \frac{\partial H}{\partial x_i} \neq 0 \text{ or } \frac{\partial H}{\partial y_i} \neq 0\}.$$

Based on these definitions, it can be checked that $\Omega = \mathcal{M} \cup \mathcal{E}$ and $\mathcal{M} \cap \mathcal{E} = 0$. For each element in $\mathcal{E}$, there exists a sensor $i \in \mathcal{N}$ such that $\frac{\partial H}{\partial x_i} \neq 0$ or $\frac{\partial H}{\partial y_i} \neq 0$. Combining this condition with the following fact $\begin{bmatrix}\cos\theta_i & \sin\theta_i\end{bmatrix}^{\mathsf{T}} \perp \begin{bmatrix}-\sin\theta_i & \cos\theta_i\end{bmatrix}^{\mathsf{T}}$, it can be concluded that $\begin{bmatrix}-\sin\theta_i & \cos\theta_i\end{bmatrix}\begin{bmatrix}\frac{\partial H}{\partial x_i} & \frac{\partial H}{\partial y_i}\end{bmatrix}^{\mathsf{T}} \neq 0$. Due to the definition of arctan$(\cdot)$ and $sign(\cdot)$, the control input ω_i is not equal to 0 and θ_i will change in such cases. As θ_i changes, the condition $\frac{\partial H}{\partial x_i}\cos\theta_i + \frac{\partial H}{\partial y_i}\sin\theta_i = 0$ is violated, which implies the set $\mathcal{E}$ is not an positive invariant set. Moreover, it is easy to check that $\mathcal{M}$ is invariant, which implies $\mathcal{M}$ is the largest invariant set in Ω. According to LaSalle's theorem [25, 33], we conclude that the state of sensors Z will converge to a point in $\mathcal{M}$ which is the same as $S_{critical}$. The conclusion is drawn. □

In implementations, when the parameter ρ_0 in Eq (4.1) is chosen small enough, $H_2(Z(t))$ usually tends to zero as $Z(t)$ converges. This implies the state $Z(t)$ usually converges into the set $\left\{Z \in \mathbb{R}^{3n} \,\middle|\, \frac{\partial H_1}{\partial Z} = 0\right\}$, which means the potential functions only slightly affect the original coverage performance determined by H_1.

7. Simulation results

7.1. Simulation results of the proposed coverage control

The numerical simulations in this section are conducted in Python software. The closed-loop system with the unicycle dynamics model in Eq (2.1) and the controllers in Eq (6.1) are numerically simulated in discrete form with a sampling period $0.1s$.

To illustrate the performance of the proposed coverage control method, simulation results with 3 and 5 mobile sensors are presented. Each sensor has the same directional sensing range with $R = 60m$ and $\alpha = \frac{4}{3}\pi$. In the performance function in Eq (2.2), D is set as 60. In the artificial potential function, η and ρ_0 are set as 0.2 and 5.0, respectively. Note that, as only numerical simulations are conducted and the sizes of the sensors are not specified, ρ is selected arbitrarily as long as it is not too large. The principles of selecting η and ρ_0 in practice are stated in Section 4.

The given area V to be covered is set as a square with coordinate X ranging from 0 to $80m$ and Y from 0 to $80m$. The coefficients in the controllers are tuned by trials, which are $k = 0.05$, $k_1 = 0.003$ and $k_2 = 0.005$. The initial states of the sensors are depicted as in Figures 3a and 4a regarding 3 and 5 sensors cases, respectively. The red disks indicate positions of the sensors, and the arrows indicate their orientations. Patches with different colours represents the covered area by different individual sensors, that is V_is, and dashed lines denote the boundaries of corresponding sensors' sensing ranges, where the same coloured patches and lines correspond to the same sensor. As declared before, a partition V_i might include several separate parts.

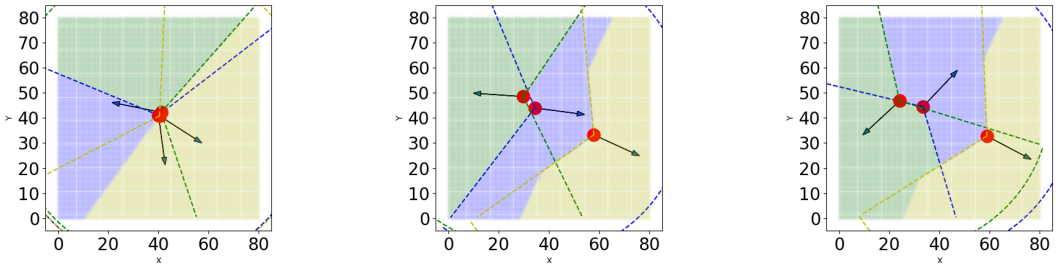

(a) $t = 0.0s$ **(b)** $t = 40.0s$ **(c)** $t = 80.0s$

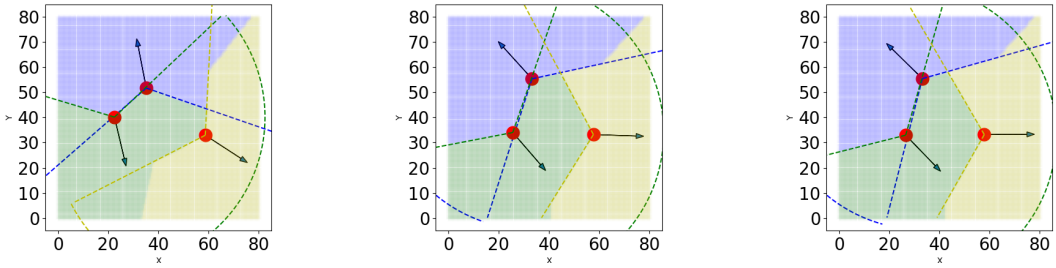

(d) $t = 120.0s$ **(e)** $t = 160.0s$ **(f)** $t = 200.0s$

Figure 3. Evolution of sensors' states over time with $\alpha = \frac{4}{3}\pi$, $n = 3$.

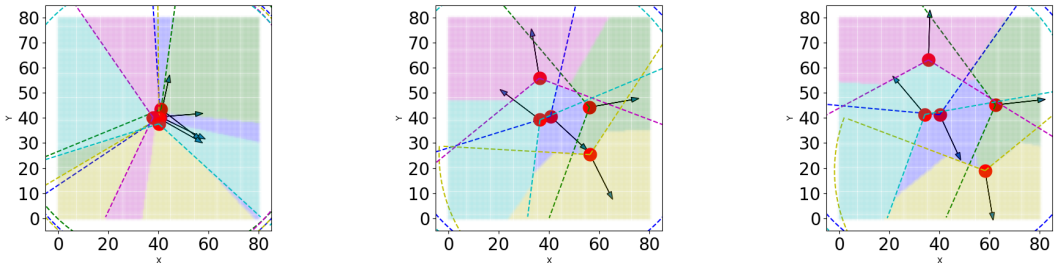

(a) $t = 0.0s$ **(b)** $t = 40.0s$ **(c)** $t = 80.0s$

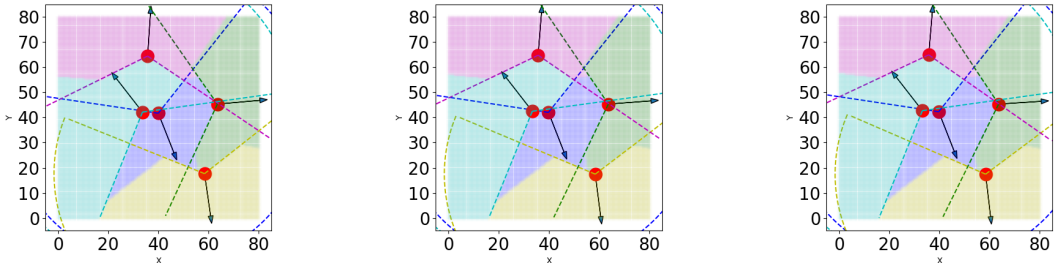

(d) $t = 120.0s$ **(e)** $t = 160.0s$ **(f)** $t = 200.0s$

Figure 4. Evolution of sensors' states over time with $\alpha = \frac{4}{3}\pi$, $n = 5$.

By implementing the control inputs as designed in Eq (6.1) and executing the controllers for $200.0s$,

the states of sensors and their coverage performance at some selected time instants are shown in Figures 3 and 4. The results imply that the states of sensors tend to be stable as time proceeding. The final coverage results in Figures 3f and 4f imply that the partition cells tend to be equally distributed over the given area , which is in line with the common sense.

The values of the overall coverage performance function $H(Z)$ evolving with time in 3 and 5 sensors' cases are depicted in Figures 5 and 6.

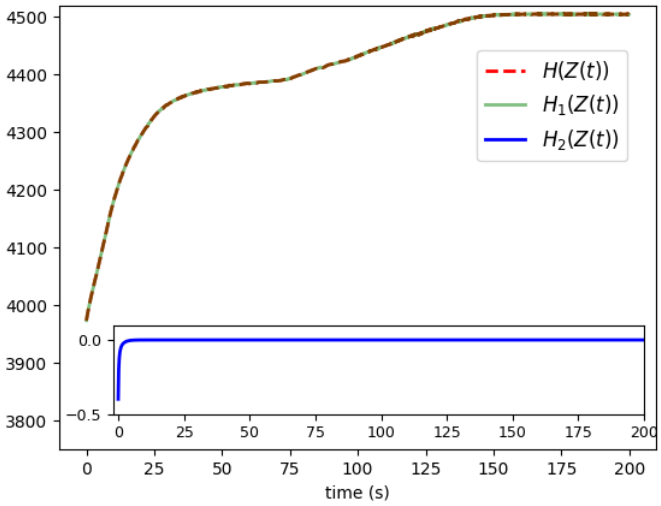

Figure 5. Values of $H(Z(t))$, $n = 3$.

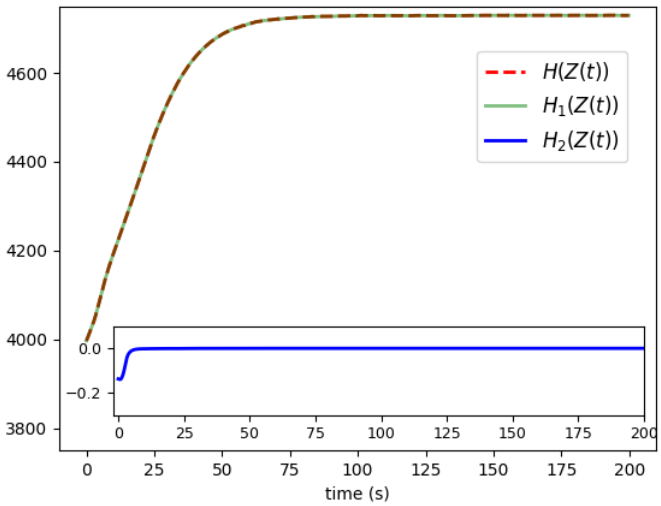

Figure 6. Values of $H(Z(t))$, $n = 5$.

It can be seen that the value function $H(Z)$ increases along the time and gradually converges to its

steady-state value. The values of $H_1(t)$ and $H_2(t)$ are also depicted in Figures 5 and 6. The values of $H_2(t)$ are very small compared to $H(Z)$ and tend to zero quickly, which implies the artificial potential function component $H_2(t)$ barely has influence on the final coverage performance of sensors.

Comparing the results with 3 and 5 sensors, the execution times do not increase with the number of sensors as the coverage control algorithm proposed is in a distribute style. Note that, it even takes more time for the 3 sensors case to converge to a critical point. The time cost of the algorithm depends on many factors such as initial states and the given area $\mathcal{V}$. However, the value of the performance function $H(Z)$ with 5 sensors is larger than with 3 sensors, which is in line with the common sense that more sensors imply a better coverage performance. As the coverage control algorithm only converge to some critical points as claimed in Theorem 2, its performance depends on initial states of the sensors. We illustrate this phenomenon by adding a simulation case still with 5 sensors but with different initial states. The initial states, final states and the values of the performance function are shown in Figures 7 and 8. Compared with Figures 4 and 6, the final states of sensors and the values of $H(Z)$ in this case are different.

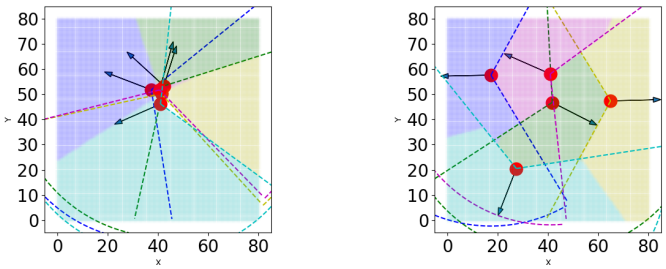

(a) $t = 0.0s$ **(b)** $t = 200.0s$

Figure 7. Evolution of sensors' states over time with $\alpha = \frac{4}{3}\pi$, $n = 5$.

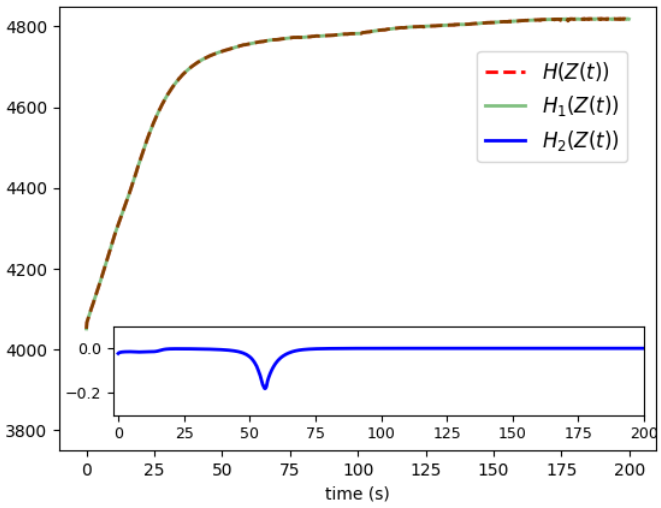

Figure 8. Values of $H(Z(t))$, $n = 5$.

7.2. Comparison with other coverage control strategies

As stated in Section 1, there are limited results [22–24] that can address the directional sensor coverage problem considered in this paper. The strategy in [22] does not consider the dead sensing zone beyond the sensing boundaries and the movement of sensors is not affected by their orientation angles, which renders the result not suitable for our problem setting. Similar concerns also exist in the strategy proposed [23]. One strategy that could properly address the proposed coverage problem is our previous work presented in [24], where performance value function $f(z_i, q)$ and boundaries $p_i a_i, p_i b_i$ are approximated in order to prevent the sensors' states from entering set S_C. In this work, $f(z_i, q)$ is approximated by $\hat{f}(z_i, q) = e^{-\frac{\sqrt{\beta(q_x - x_i)^2 + (q_y - y_i)^2}}{D}} \mathbf{1}_{S_i}(q)$, and $p_i a_i, p_i b_i$ are approximated by $\widehat{p_i a_i} : \begin{bmatrix} x & y \end{bmatrix}^\mathsf{T} := \Re(\theta_i + \frac{\alpha}{2}) \begin{bmatrix} \tau & \frac{-\gamma}{1+e^{-\tau}} \end{bmatrix}^\mathsf{T} + p_i$, $\widehat{p_i b_i} : \begin{bmatrix} x & y \end{bmatrix}^\mathsf{T} := R(\theta_i - \frac{\alpha}{2}) \begin{bmatrix} \tau & \frac{\gamma}{1+e^{-\tau}} \end{bmatrix}^\mathsf{T} + p_i, \tau \in [0, R)$.

By choosing $\beta = 0.9$ and $\gamma = 0.2$ and making other settings the same as in the simulation case in Figure 4f, the simulation results using the control algorithm in [24] are depicted in Figures 9 and 10.

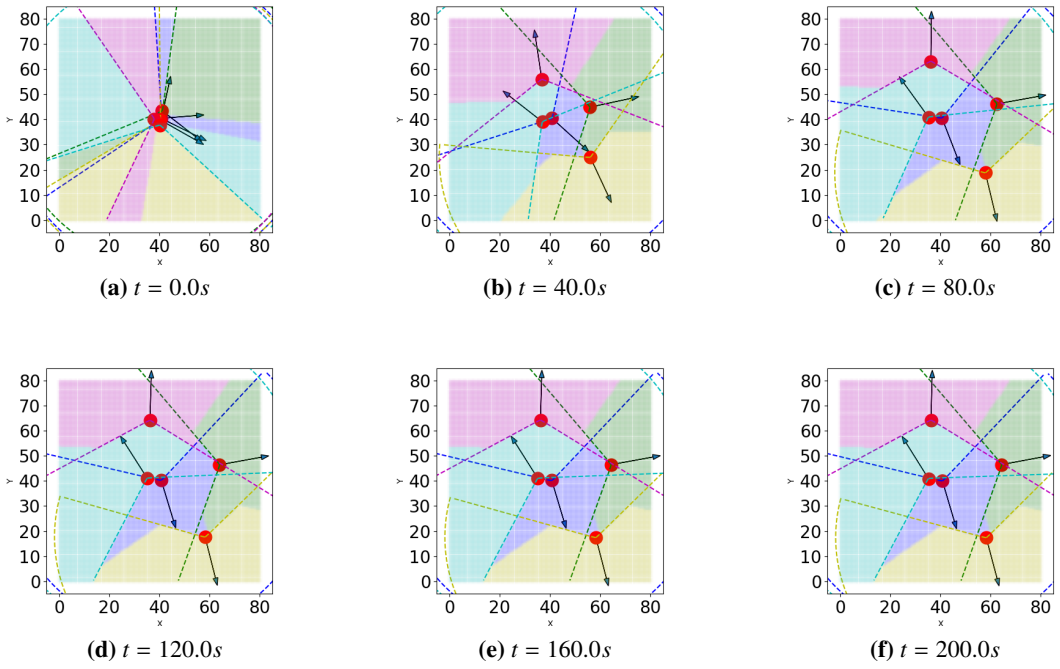

(a) $t = 0.0s$ **(b)** $t = 40.0s$ **(c)** $t = 80.0s$

(d) $t = 120.0s$ **(e)** $t = 160.0s$ **(f)** $t = 200.0s$

Figure 9. Evolution of sensors' states over time with $\alpha = \frac{4}{3}\pi$, $n = 5$, $\beta = 0.99$, $\gamma = 0.01$.

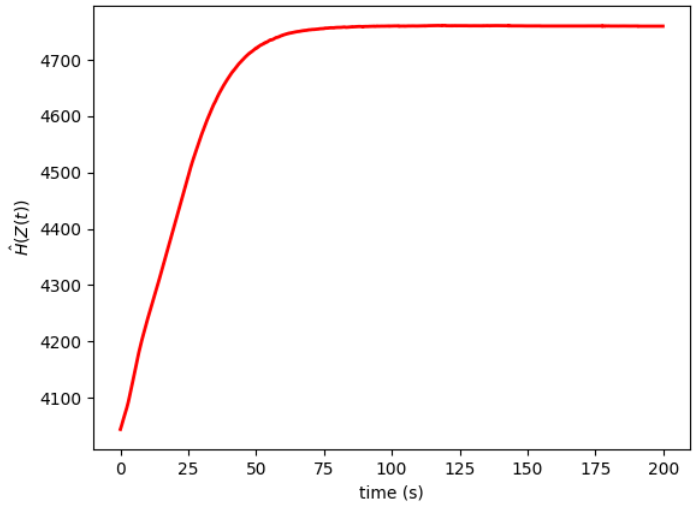

Figure 10. Values of $\hat{H}(Z(t))$.

Comparing the results in Figures 4, 6, 9 and 10, the coverage performances of the two methods are similar. Note that approximations used in [24] have negative influence on coverage performance though slightly. Moreover, due to the approximation of boundaries, computation of the corresponding gradients is more complex than the proposed approach in this paper.

8. Conclusions

In this paper, coverage control using directional mobile sensors with non-linear dynamics and non-smooth sensing ranges is considered. The dynamics of each sensor is modelled by a unicycle model while the sensing range of each sensor is modelled as a circular sector. Within the sensing ranges, the coverage performance value is determined by the distances and orientation angles of the sensors. Moreover, potential functions penalizing the distances between sensors are incorporated into coverage performance valuation function, which renders the gradient of the coverage performance function well-defined along the trajectory of the closed-loop system. Based on the gradient of the performance value function, a novel non-smooth coverage controller is proposed for sensors and its convergence property is analysed. Simulation results are provided to illustrate the performance of the proposed coverage control strategy. As there are oscillations caused by the non-smooth property of the closed-loop system and the discretization in implementation, a future direction of this work is to analyse the discrete implementation of the coverage controller to mitigate this phenomenon. In the proposed control strategy, the communication between neighbouring sensors is assumed to be perfect. However, imperfect communication is a commonly encountered problem in practical applications and should be addressed in controller development as pointed in [34, 35]. Thus, coverage control with addressing imperfect communication links is a future direction of this work. Moreover, to alleviate the computation burden in calculating gradients and address a more practical sensing performance, some model-free gradient estimation based control methods, such as extremum seeking strategy, can be exploited in coverage control design.

Acknowledgments

This work was supported in part by Defense Industrial Technology Development Program.

Conflict of interest

The authors declare there is no conflict of interest.

References

1. X. Wang, H. Zhang, S. Fan, H. Gu, Coverage control of sensor networks in iot based on rpso, *IEEE Int. Things J.*, **5** (2018), 3521–3532. https://doi.org/10.1109/JIOT.2018.2829160
2. G. M. Atınç, D. M. Stipanović, P. G. Voulgaris, A swarm-based approach to dynamic coverage control of multi-agent systems, *Automatica*, **112** (2020), 108637. https://doi.org/10.1016/j.automatica.2019.108637
3. B. Wang, *Coverage control in sensor networks*, Springer Science & Business Media, 2010.
4. S. Meguerdichian, F. Koushanfar, M. Potkonjak, M. B. Srivastava, Coverage problems in wireless ad-hoc sensor networks, in *Proceedings IEEE INFOCOM 2001. Conference on Computer Communications. Twentieth Annual Joint Conference of the IEEE Computer and Communications Society (Cat. No. 01CH37213)*, (2001), 1380–1387. https://doi.org/10.1109/INFCOM.2001.916633
5. C. F. Huang, Y. C. Tseng, The coverage problem in a wireless sensor network, *Mob. Netw. Appl.*, **10** (2005), 519–528. https://doi.org/10.1007/s11036-005-1564-y
6. G. M. Atınç, D. M. Stipanović, P. G. Voulgaris, A swarm-based approach to dynamic coverage control of multi-agent systems, *Automatica*, **112** (2020), 108637. https://doi.org/10.1016/j.automatica.2019.108637
7. W. Bentz, T. Hoang, E. Bayasgalan, D. Panagou, Complete 3-d dynamic coverage in energy-constrained multi-uav sensor networks, *Auton. Robots*, **42** (2018), 825–851. https://doi.org/10.1007/s10514-017-9661-x
8. F. Abbasi, A. Mesbahi, J. M. Velni, A new voronoi-based blanket coverage control method for moving sensor networks, *IEEE Trans. Control Syst. Technol.*, **27** (2019), 409–417. https://doi.org/10.1109/TCST.2017.2758344
9. W. Luo, K. Sycara, Voronoi-based coverage control with connectivity maintenance for robotic sensor networks, in *2019 International Symposium on Multi-Robot and Multi-Agent Systems (MRS)*, 2019, 148–154. https://doi.org/ 10.1109/MRS.2019.8901078
10. D. Inoue, Y. Ito, H. Yoshida, Optimal transport-based coverage control for swarm robot systems: Generalization of the voronoi tessellation-based method, *IEEE Control Syst. Lett.*, **5** (2021), 1483–1488. https://doi.org/ 10.1109/LCSYS.2020.3039008
11. S. Martinez, J. Cortes, F. Bullo, Motion coordination with distributed information, *IEEE Control Syst. Mag.*, **27** (2007), 75–88. https://doi.org/ 10.1109/MCS.2007.384124

12. Q. An, Y. Shen, Distributed coverage control for mobile camera sensor networks with anisotropic perception, *IEEE Sens. J.*, **21** (2021), 16264–16274. https://doi.org/10.1109/JSEN.2021.3075627

13. J. Cortes, S. Martinez, T. Karatas, F. Bullo, Coverage control for mobile sensing networks, *IEEE Trans. Robot. Autom.*, **20** (2004), 243–255. https://doi.org/10.1109/TRA.2004.824698

14. S. Poduri, G. S. Sukhatme, Constrained coverage for mobile sensor networks, in *IEEE International Conference on Robotics and Automation*, 2004, 165–171. https://doi.org/10.1109/ROBOT.2004.1307146

15. J. Cortes, S. Martinez, F. Bullo, Spatially-distributed coverage optimization and control with limited-range interactions, *ESAIM: Control, Optimisat. Calculus Var.*, **11** (2005), 691–719. https://doi.org/10.1051/cocv:2005024

16. M. Santos, Y. Diaz-Mercado, M. Egerstedt, Coverage control for multirobot teams with heterogeneous sensing capabilities, *IEEE Robot. Autom. Lett.*, **3** (2018), 919–925. https://doi.org/10.1109/LRA.2018.2792698

17. Y. Kantaros, M. Thanou, A. Tzes, Distributed coverage control for concave areas by a heterogeneous robot–swarm with visibility sensing constraints, *Automatica*, **53** (2015), 195–207. https://doi.org/10.1016/j.automatica.2014.12.034

18. Y. Stergiopoulos, A. Tzes, Coverage-oriented coordination of mobile heterogeneous networks, in *2011 19th Mediterranean Conference on Control & Automation (MED)*, 2011, 175–180. https://doi.org/10.1109/MED.2011.5983132

19. M. T. Nguyen, L. Rodrigues, C. S. Maniu, S. Olaru, Discretized optimal control approach for dynamic multi-agent decentralized coverage, in *2016 IEEE International Symposium on Intelligent Control (ISIC)*, 2016, 1–6. https://doi.org/10.1109/ISIC.2016.7579984

20. J. Cortés, F. Bullo, Nonsmooth coordination and geometric optimization via distributed dynamical systems, *SIAM Rev.*, **51** (2009), 163–189. https://doi.org/10.1137/080737551

21. M. A. Guvensan, A. G. Yavuz, On coverage issues in directional sensor networks: A survey, *Ad. Hoc. Networks*, **9** (2011), 1238–1255. https://doi.org/10.1016/j.adhoc.2011.02.003

22. X. Zhang, X. Chen, X. Liang, Y. Fang, Distributed coverage optimization for deployment of directional sensor networks, in *2015 54th IEEE Conference on Decision and Control (CDC)*, (2015), 246–251. https://doi.org/10.1109/CDC.2015.7402116

23. Y. Stergiopoulos, A. Tzes, Cooperative positioning/orientation control of mobile heterogeneous anisotropic sensor networks for area coverage, in *2014 IEEE International Conference on Robotics and Automation (ICRA)*, (2014), 1106–1111. https://doi.org/10.1109/ICRA.2014.6906992

24. Z. Ju, Y. Tan, H. Zhang, X. Chen, Coverage control using directional nonlinear dynamic sensors with non-smooth sensing range, in *2020 59th IEEE Conference on Decision and Control (CDC)*, (2020), 5309–5314. https://doi.org/10.1109/CDC42340.2020.9303906

25. A. Astolfi, Exponential stabilization of a wheeled mobile robot via discontinuous control, *J. Dyn. Syst., Meas., Control*, **121** (1999), 121–126. https://doi.org/10.1115/1.2802429

26. X. Li, Y. Tan, I. Mareels, X. Chen, Compatible formation set for uavs with visual sensing constraint, in *2018 Annual American Control Conference (ACC)*, (2018), 2497–2502. https://doi.org/10.23919/ACC.2018.8431269
27. M. T. Nguyen, L. Rodrigues, C. S. Maniu, S. Olaru, Discretized optimal control approach for dynamic multi-agent decentralized coverage, in *2016 IEEE International Symposium on Intelligent Control (ISIC)*, (2016), 1–6. https://doi.org/10.1109/ISIC.2016.7579984
28. R. Klein, *Concrete and abstract Voronoi diagrams*, Springer Science & Business Media, 1989.
29. H. Flanders, Differentiation under the integral sign, *Am. Math. Mon.*, **80** (1973), 615–627. https://doi.org/10.1080/00029890.1973.11993339
30. R. W. Brockett, *Control Theory and Singular Riemannian Geometry*, New York, NY, 1982. https://doi.org/10.1007/978-1-4612-5651-9_2
31. D. Shevitz, B. Paden, Lyapunov stability theory of nonsmooth systems, *IEEE Trans. Autom. Control*, **39** (1994), 1910–1914. https://doi.org/10.1109/9.317122
32. A. F. Filippov, *Differential Equations with Discontinuous Righthand Sides: Control Systems*, Springer Science & Business Media, 2013.
33. H. K. Khalil, *Nonlinear Systems*, Prentice Hall, 2002.
34. Z. Ye, D. Zhang, Z. G. Wu, H. Yan, A3c-based intelligent event-triggering control of networked nonlinear unmanned marine vehicles subject to hybrid attacks, *IEEE Trans. Intell. Trans. Syst.*, 1–14. https://doi.org/10.1109/TITS.2021.3118648
35. D. Zhang, Z. Ye, G. Feng, H. Li, Intelligent event-based fuzzy dynamic positioning control of nonlinear unmanned marine vehicles under dos attack, *IEEE Trans. Cybern.*, 1–14. https://doi.org/10.1109/TCYB.2021.3128170

AIMS Press